Rapid Continental Subsidence Following the Initiation and Evolution of Subduction

Michael Gurnis

Dynamic topography resulting from initiation of slab subduction at an ocean-continent margin causes the continental lithosphere to subside rapidly. As subduction continues and the slab shallows, a basin depocenter and forebulge migrate in toward the continental interior. Finally, closure of the ocean basin leads to regional uplift. These active margin processes have commonly been ascribed to supracrustal loading, but numerical modeling shows that dynamic subsidence rates can exceed 100 meters per million years and are similar to rates of sediment accumulation along convergent North American plate margins over the Phanerozoic.

Following the recognition nearly a century ago that kilometer-thick sedimentary deposits commonly lie interior to continental margins [later named geosynclines (*1*)], it was realized that crustal downwarping must have accompanied or preceded deposition. The origin of such subsidence was much debated (*2*), but it was also realized early on that because these basins are partly filled with coarse clastic sediments and volcanic rocks, their origins must be associated with orogenesis. A model has become widely accepted in which orogenic and fold-thrust belts (*3*), which lie on top of the lithosphere, elastically bend the continent downward at converging plate boundaries. Such downwarping by these supracrustal loads may lead to the development of foreland basins that are infilled by sediments shed from the adjacent topographic loads (*4*).

At ocean-continent converging margins, oceanic lithosphere subducting under the continent is also a load. Viscous flow models have shown that the presence of slabs, which are colder than average mantle, causes surface depressions (dynamic topography) of nearly 1 km (*5, 6*). Furthermore, any change in the characteristics of subduction will lead to a change in buoyancy and hence to fluctuations in the magnitude and shape of dynamic topography (*6, 7*). It therefore follows that changes in subduction can lead directly to uplift or subsidence of an overriding continent. On the basis of the distribution of volcanic rocks [for example (*8*)], it has been suggested that a progressive decrease in the dip of the subducting oceanic crust (*6, 9*) caused excessive (*10*) Late Cretaceous submergence of western North America and that subsequent cessation of subduction led to broad-scale Cenozoic uplift (*6, 11*). In this report I show that the normal evolution of slabs, and especially the initiation of subduction, can lead to high rates of subsidence over large length scales.

Department of Geological Sciences, 1006 C. C. Little Building, University of Michigan, Ann Arbor, MI 48109.

New subduction zones probably must form where the oceanic lithosphere is old so that the strength of the lithosphere can be overcome (*13*). The oceanic lithosphere may even reach its greatest age and density just before the initiation of subduction. Descending into the upper mantle, the new slab will cause the continental lithosphere to rapidly subside. On the basis of estimates of typical plate subsidence and age, an order of magnitude estimate of subsidence rate is readily derived. Oceanic lithosphere subsides about 3 km in 160 million years (m.y.) as it cools (*14*). If this dense lithosphere were now at depth in the viscous mantle, instead of lying isostatically near the Earth's surface, the dynamic topography resulting from this load would be attenuated. However, for a load at a depth of 200 km, this attenuation would not be significant (*15*). For an oceanic plate subducting at 5 cm/year, most of the change in dynamic topography occurs while the slab initially moves through the upper mantle, in less than about 10 m.y. A 3-km dynamic subsidence in 10 m.y., together with sediment loading, will give an apparent subsidence of about 500 m per million years—as large as the largest apparent subsidence observed on the North American craton during the Phanerozoic (*16*). This is a crude upper limit but clearly shows that the initiation of subduction must be a significant factor in controlling subsidence along continental margins. Because amounts of subsidence will depend on subduction geometry, age of the oceanic plate, and rheology of the mantle, a dynamic viscous model must be used to predict the dynamics of such convergent systems. Therefore, I developed models of the subduction environment with strong horizontal and vertical variations in viscosity that allow for the computation of synthetic stratigraphy along a continental margin from the initiation of subduction through closure of an ocean basin.

The two-dimensional numerical model (some details in Fig. 1) has a total width of 6000 km and a depth of 1500 km. A trench is placed close to the center of the computational domain, and the fluid interior has a high-viscosity lithosphere, a low-viscosity zone, an upper and lower mantle, and a high-viscosity slab. The thickness of the lithosphere jumps at the ocean-continent boundary. Overlying the continental lithosphere is an elastic lid of uniform rigidity that is free at the continent boundary in order to simulate a fault in the elastic lithosphere. The descending slab has a uniform temperature equal to the average temperature of the lithosphere subducting with an age, τ_s (*17*). Only the equation of motion of a slow creeping fluid is solved (*18*); time dependence is simulated with a sequence of different slab configurations. Stress of the dense slab is transmitted by viscous flow to the surface. The total vertical stress on the top loads the elastic lid and results in dynamic topography (*19*). Space between dynamic topography and sea level (set to a constant value of zero) is filled with sediments, and a stratigraphic cross section is created by sequentially changing slab configurations.

For a model with a slab at a depth of 600 km, a dip of 80°, and an age of 160 m.y., there is little difference between the raw topography from the viscous stress and the loading of the elastic lid at this relatively long wavelength. A prominent ~25-m-high forebulge developed at 400 km from the ocean-continent boundary. This forebulge was controlled by viscous flow. The obliquely descending slab with a finite length resulted in a counter flow with strong upwelling; in the presence of a low-viscosity zone and a high-viscosity lithosphere and slab, the topography bulged upward over the upwelling (*20*). Both deeper and shallower dipping slabs excite longer wavelength counter flows and thus cause the bulge to be pushed farther in toward the continental interior.

A fundamental ambiguity in assessing vertical motions associated with subduction is our poor understanding of the time evolution of slab structure, especially that just following the initiation of subduction. Dynamic models of plates and convection in which slabs are entirely free to adjust to the dynamics of the system show that slabs descend vertically through the upper mantle following the initiation of subduction (*21*). However, slab dip shallows as a horizontal pressure gradient develops (*22*), and it may take about 50 m.y. to bring a vertical slab to an asymptotic dip of about 45° (*21*). Slabs in the western Pacific approximate this trend (*21*): the two youngest slabs, Mariana and Kermadec, are nearly vertical, whereas the oldest slab, Japan, has a shallow dip near 45° (*23*). To approximate this evolutionary trend, I modeled a slab that shallowed in 50 m.y.

Three phases were evident in the evolution of the ocean basin (Fig. 2) associated with (i) initiation of subduction, (ii) rapid shallowing of slab dip, and (iii) closure of the ocean basin. These three phases are distinguished not only by slab and lithosphere geometry but also by time scale: the first phase occurred in ~10 m.y., the second in ~50 m.y., and the third in ~150 m.y. During initiation of subduction (Fig. 2A), the rate of subsidence decreased as the leading edge of the slab descended to greater depths and to greater distances from the continental surface. The resulting basin was some 200 km in width and had a well-developed forebulge. As the slab descended through the upper mantle, the viscous forebulge migrated toward the continental interior, and sediments progressively lapped onto previously uplifted regions. The maximum rate of subsidence was about 200 m per million years and was dependent on the distance between the trench and the ocean-continent boundary. Here, the distance was a conservative 150 km, but if the trench and ocean-continent boundary overlap, then the maximum rate of subsidence would be 400 m per million years for 160-million-year-old oceanic lithosphere. If the slab descends obliquely then the rate of subsidence can be even higher.

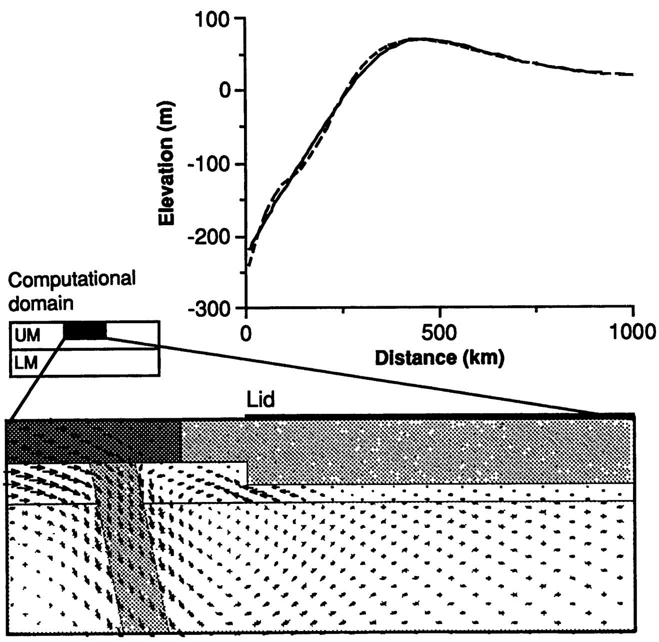

Fig. 1. Schematic of the finite-element model in the vicinity of the slab (*37*). Overlying the continental lithosphere are two profiles of topography not yet loaded by sediment: the raw dynamic topography (dashed line) and the dynamic topography that loads the elastic plate (solid line). In the lower panel, shading denotes units of different viscosity: upper right is continental lithosphere, η_C; upper left is oceanic lithosphere, η_{OL}; the slab, η_S; the unshaded region just below the lithosphere is the low-viscosity zone, η_{LVZ}; and below the LVZ is the upper mantle, η_{UM}. The thick horizontal line on top of the continental lithosphere is the elastic lid. Only every third velocity vector is plotted. The mesh is most refined in the low-viscosity zone near the slab. The viscosities are $\eta_C = 10^{23}$ Pa-s, $\eta_O = 10^{21}$ Pa-s, $\eta_{LVZ} = 10^{19}$ Pa-s, $\eta_{UM} = 10^{21}$ Pa-s, and $\eta_{LM} = 10^{23}$ Pa-s. The viscosity of the slab is 10^2 times as large as adjacent layers in the LVZ, for example, $\eta_S = 10^{21}$ Pa-s).

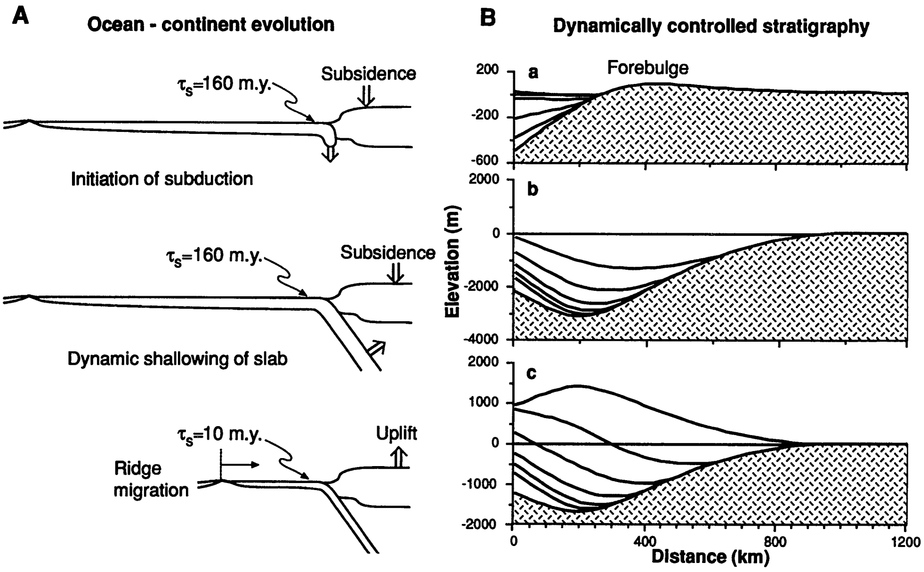

Fig. 2. Plate and slab configuration during three stages of the evolution of a subduction zone (on the left) and the cumulative stratigraphy that results since the initiation of subduction (on the right). On the right, the thick solid lines are chronostratigraphic surfaces, the horizontal line is the sea level, and the line underlain by the stippling is the original land surface before subduction was initiated. During the first phase (**A**), chronostratigraphic surfaces are shown for a slab that successively deepens by 100 km. For a slab that descends at 5 cm/year, these 100-km slab depth intervals correspond to 2 m.y. chronostratigraphic surfaces. During the second phase (**B**), the vertical distance between chronostratigraphic surfaces increases for each 10° decrease in slab dip.

During the second phase (Fig. 2B) the slab shallowed, and in the example shown the age of the oceanic lithosphere subducting (τ_s) is 160 m.y. (*24*). As slab dip decreased, both the amplitude and width of the depression increased as the basin center migrated toward the continental interior. Although the second phase occurred over a much longer period of time (50 m.y.), the overall magnitude of subsidence was substantially higher than that which occurred during the initial phase. Apparent subsidence rates of the order 100 m per million years were somewhat less than those found during the initiation of subduction and were directly proportional to the rate at which the slab dip angle decreased. As the center of dynamic topography migrated inward, the continental surface nearest the trench rebounded; as a result, sedimentary sequences were uplifted and tilted. Like the initiation phase, a shallowing dip phase also resulted in a forebulge that migrated toward the continental interior. Significantly, as the slab shallowed, continental crust, which previously bowed upward, became covered with sediment as the magnitude of the depression increased and the depocenter advanced toward the interior of the continent.

During the third and final phase, the ocean basin closed. In so doing the age of the oceanic lithosphere decreased and, for a slab at both a constant depth and dip, there was a dramatic uplift of the continent in the model (*6*). The effect where τ_s decreased from 160 to 10 m.y. was to create a plateau 800 km across, more than 1 km high, and with tilted stratigraphic horizons (Fig. 2C). The rate of uplift was directly proportional to the rate at which the oceanic ridge and trench converged. For an initial ridge to trench distance of 7000 km and a convergence of 5 cm/year, this uplift was only 10 m per million years.

The model of margin evolution just discussed (Fig. 2) can be compared to the classic Wilson cycle, the Cambrian to Devonian evolution of Iapetus. During the Cambrian and Early Ordovician, the northeastern Laurentia margin was passive, forming perhaps after the breakup of an Eocambrian supercontinent (*25*). During the middle Ordovician, nearly coeval with the initiation of subduction off the east coast of Laurentia (*26*) but before the Taconic uplift on the eastern margin, continental crust was tilted downward in a broad zone 200 to 500 km wide (*27, 28*). Later, during the Late Ordovician and Silurian, the Queenston clastic wedge was shed off of the Taconic uplift (*27, 28*). But rapid drowning of the continent preceded deposition of this clastic wedge; in Quebec (*29*), eastern Pennsylvania (*30*), and eastern Tennessee (*30, 31*) subsidence was so rapid that deposition could not keep up with rates of subsidence, which exceeded 50 m per million years (*16, 30, 31*). In order to explain such subsidence without a supracrustal load, it has been suggested that tilting of the Laurentian margin was driven by partial subduction of continental crust into an eastward dipping subduction zone (*30*). Polarity of the post mid-Ordovician subduction zone is uncertain, but may well have been westward dipping (*32*), as implied by the rapid pre-Taconic uplift. During this time, uplift and the development of regional unconformities preceded subsidence of the margin (*30, 33*). Rapid subsidence is expected during the initiation of subduction (Fig. 2A) and such uplift and development of unconformities are predicted by the viscous slab models as a viscous forebulge that migrates in toward the continental interior.

The model assumption that rate of deposition keeps up with subsidence is probably not exactly correct because dynamic subsidence rates generated by the slab are so high. A more realistic sedimentation rate would have two effects: first, it would reduce calculated subsidence rates and make them closer to observed values in the range of 10 to 50 m per million years (*16*). Second, the calculated sediment thickness would be reduced, and this ultimately would lead to a much smaller plateau as the ocean basin closed. Lesser sequence thicknesses may account for the lack of significant regional uplift (*28*) following the Devonian closure of Iapetus.

The numerical models are broadly consistent with the pre-Taconic evolution of eastern Laurentia, but because the record of vertical motion has been obscured by subsequent orogenesis, it is beneficial to apply the model to more recent events where either plate convergence or plate geometry has fluctuated. Already alluded to is the decrease in age of the subducting Farallon plate and its eventual Tertiary demise. The Cenozoic uplift of western North America is consistent with these (Fig. 2C) and earlier models (*6, 11*). An additional example occurs in the western Pacific where the age of the oceanic lithosphere subducting has been increasing since the late Mesozoic. The slab subducting from Indonesia to Japan is currently greater than 100 million years old, but during the Cretaceous the age of the oceanic lithosphere just before subduction may have only been 40 to 80 million years old (*34*). Consequently, we would expect active subsidence of continental crust just above these slabs. Currently, continental crust behind western Pacific trenches from Indonesia to Alaska is submerged at shallow water depths (*35*).

Perhaps most importantly, these models have been created in isolation from the effects of supracrustal loads and eustatic sea level fluctuations. Clearly, supracrustal loads over the long term would act in concert with the slab effects, although there may be an initial short-term phase offset. Moreover, change in rates of subduction is ultimately caused by change in the rates of sea floor spreading, and the combination of spreading and subduction can lead to complex phase offsets between eustatic and epeirogenic effects (7). Orogenic, epeirogenic, and eustatic processes are closely coupled (*36*), and these and other models (7) allow better understanding of the ultimate dynamic interrelationships among the three.

REFERENCES AND NOTES

1. M. Kay, *Geol. Soc. Am. Mem.* **48**, 1 (1951).
2. R. H. Dott, *Soc. Econ. Paleontol. Mineral. Spec. Publ.* **19**, 1 (1974).
3. R. A. Price, in *Gravity and Tectonics*, K. A. DeJong and R. Schoten, Eds. (Wiley, New York, 1973), pp. 491–502.
4. C. Beaumont, *Geophys. J.* **65**, 291 (1980).
5. B. H. Hager, *J. Geophys. Res.* **89**, 6003 (1984).
6. A. X. Mitrovica, C. Beaumont, G. T. Jarvis, *Tectonics* **8**, 1079 (1989).
7. M. Gurnis, *Science* **250**, 970 (1990).
8. W. R. Dickinson and W. S. Snyder, *Geol. Soc. Am. Mem.* **151**, 355 (1978).
9. T. H. Cross and R. H. Pilger, *Nature* **274**, 653 (1978).
10. G. Bond, *Geology* **4**, 557 (1976).
11. Before the recognition of viscous dynamic topography, P. E. Damon [*Tectonophysics* **61**, 307 (1979)] realized the importance of slabs on vertical motion of the crust from isostatic considerations.
12. J. T. Wilson, *Nature* **211**, 676 (1966).
13. D. P. McKenzie, in *Island Arcs, Deep Sea Trenches, and Back-Arc Basins*, M. Talwani and W. C. Pittman, Eds. (American Geophysical Union, Washington, DC, 1977), pp. 57–61. In an alternative model, it is assumed that subduction is initiated when the oceanic lithosphere is young [S. Cloetingh, R. Wortel, N. J. Vlaar, *Pure Appl. Geophys.* **129**, 7 (1989)].
14. J. G. Sclater, C. Jaupart, D. Galson, *Rev. Geophys. Space Phys.* **18**, 268 (1980).
15. B. Parsons and S. Daly, *J. Geophys. Res.* **88**, 1129 (1983).
16. L. L. Sloss, in *Sedimentary Cover—North American Craton: U.S.*, vol. D-2 of *The Geology of North America*, L. L. Sloss, Ed. (Geological Society of America, Denver, CO, 1988)), pp. 25–51.
17. The average temperature difference between slab and mantle is $2(T_s - T_m)(\kappa\tau_s/\pi)^{1/2}/L_o$, where T_s and T_m are the surface and mantle temperatures (273 K and 1673 K), respectively, κ is the thermal diffusivity (10^{-6} m^2 s^{-1}), and L_o is the thickness of the oceanic lithosphere (100 km).
18. S. D. King, A. Raefsky, B. H. Hager, *Phys. Earth Planet. Int.* **59**, 195 (1990).
19. A. B. Watts and S. F. Daly, *Annu. Rev. Earth Planet. Sci.* **9**, 415 (1981).
20. Because topography has not been investigated with such realistic viscosity variations, a forebulge has not previously been observed. Although the bulge amplitude is dependent on all aspects of the viscosity distribution, it is primarily dependent on the finite length of the slab and the characteristics of the low-viscosity zone and lithosphere. It is negligibly dependent on the boundary conditions of the side walls.
21. M. Gurnis and B. H. Hager, *Nature* **335**, 317 (1988).
22. The angle of subduction is probably controlled by a balance between the vertical buoyancy of the slab and the horizontal pressure gradient generated by obliquely dipping slabs [D. J. Stevenson and J. S. Turner, *Nature* **270**, 334 (1977)]. During the initial, nearly vertical descent through the upper mantle, there is no substantial pressure gradient.
23. The age of the slab, defined as the time since subduction was initiated, is based upon the oldest surviving rocks in the volcanic arc [R. D. Jarrard, *Rev. Geophys. Space Phys.* **24**, 217 (1986)]; this provides a lower limit to the age of the slab.
24. It is probably more realistic to decrease slab age while the dip decreases, but the topographic effect of decreasing slab age is small in comparison to decreasing slab dip over a 50 m.y. period for 160-million-year-old lithosphere.
25. G. C. Bond, P. A. Nickelson, M. A. Kominz, *Earth Planet. Sci. Lett.* **70**, 325 (1984).
26. J. M. Bird and J. F. Dewey, *Geol. Soc. Am. Bull.* **81**, 1031 (1970).
27. P. B. King, *Evolution of North America* (Princeton Univ. Press, Princeton, NJ, 1959).
28. T. D. Cook and A. W. Bally, *Stratigraphic Atlas of North and Central America* (Princeton Univ. Press, Princeton, NJ, 1975).
29. R. N. Hiscott, *Can. J. Earth Sci.* **15**, 1579 (1978).
30. G. Shanmugan and G. G. Lash, *Geology* **10**, 562 (1982).
31. G. L. Benedict, K. R. Walker, *Am. J. Sci.* **278**, 579 (1978).
32. Most models of early Appalachian tectonics have an eastern dipping slab [for example, (*26*) and R. D. Hatcher, in *The Appalachian-Ouachita Orogen in the United States*, vol. F-2 of *Geology of North America*, R. D. Hatcher, W. A. Thomas, G. W. Viele, Eds. (Geological Society of America, Denver, CO, 1988), pp. 511–535], but this slab is generally assumed to be attached to a small marginal basin plate. The major slab probably was westward dipping [B. A. van der Pluijm, R. J. E. Johnson, R. Van der Voo, *Geology* **18**, 898 (1990)].
33. R. D. Jacobi, *Earth Planet. Sci. Lett.* **56**, 245 (1981); I. Knight, N. P. James, T. E. Lane, *Geol. Soc. Am. Bull.* **103**, 1200 (1991).
34. T. W. C. Hilde, S. Uyeda, L. Kroenke, *Tectonophysics* **38**, 145 (1977). This tectonic reconstruction is speculative because most magnetic lineations recording the event have since subducted.
35. M. Gurnis, *Eos* **72**, 271 (1991).
36. J. G. Johnson, *Geol. Soc. Am. Bull.* **82**, 3263 (1971).
37. Additional parameters of the model include: the coefficient of thermal expansion, 2×10^{-5} K^{-1}; the ambient density of the upper mantle, 3500 kg m^{-3}; and flexural rigidity of the continental plate, 5.0×10^{23} N-m.

38. Acknowledgment is made to the donors of The Petroleum Research Fund, administered by the American Chemical Society, for partial support of this research. Also supported by NSF grants EAR-8957164 and EAR-8904660. B. Wilkinson made detailed comments which substantially improved this manuscript.

22 October 1991; accepted 31 January 1992